International Atomic Energy Agency

INDC(IAE)-004/G
IAEA/RL/26

INDC INTERNATIONAL NUCLEAR DATA COMMITTEE

The disintegration of $^{103}Rh^{m}$

K.H. Czock

N. Haselberger

F. Reichel

International Atomic Energy Agency
Vienna

September 1974

IAEA NUCLEAR DATA SECTION, KÄRNTNER RING 11, A-1010 VIENNA

INDC(IAE)-004/G
IAEA/RL/26

The disintegration of $^{103}Rh^{m}$

K.H. Czock

N. Haselberger

F. Reichel

International Atomic Energy Agency
Vienna

September 1974

The disintegration of $^{103}Rh^{m}$.

ABSTRACT

A technique for determination of the disintegration rate of $^{103}Rh^{m}$ in thick foils is described.

In addition values for the following parameters were determined:

- total internal conversion coefficient
  $\alpha = 1531 \pm 30$,

- K shell internal conversion coefficient $\alpha_K = 127 \pm 6$

- conversion ratio $R = \frac{K}{L + M + \ldots} = 0.0914 \pm 0.0043$

INTRODUCTION

The utilization of the $^{103}Rh(n,n')^{103}Rh^{m}$ reaction for fast neutron flux and dose determinations depends on the knowledge of the excitation function and reaction rate determination. Many papers have been published on this subject (1-12).

Because all the reported cross section data have been obtained by the activation technique, a special care has to be taken in the activity determination (13). There is no simple way to obtain the absolute activity in a rhodium foil from the measured counting rate. Since the previously reported nuclear data (α_k, α) are not in agreement with observations here, a re-determination seemed worthwhile.

$^{103}Rh^{m}$ decays to the ground state with a half-life of 56,116 min (14) and a transition energy of 39,75 keV. This isomeric level is strongly converted. The activity can, therefore, be obtained by measuring either the electrons or the X-rays produced in the conversion. The 20 keV X-rays are the most convenient for this measurement.

Determination of rhodium activity

The detector for counting rhodium activity is an integral assembly of a NaI(Tl) crystal (38 mm diameter x 2 mm thickness) and a beryllium window ($\sim$ 0,125 mm thick). The counter is shielded with 10 cm of lead for background reduction. The pulse height spectrum is displayed on a multichannel analyzer. The efficiency of the detector for the 20 keV K X-rays was determined with calibrated sources of $^{103}Rh^{m}$ electro-deposited on VYNS films. The disintegration rate of these sources was determined by $4\pi e$-X coincidence technique. The efficiency of the 4π counter for the 17 keV K-conversion electrons was 99,5%.

A detailed description of the 4πe–X calibration and source preparation from a Pd–Rh generator is given elsewhere (15,16).

In this way the X-ray detector calibration for 4 detector–to–source distances (see Table I) was obtained independently of the conversion factors (α, α_K) and fluorescence yield ω_k values.

$$N_i = \varepsilon_i \cdot N_o = \frac{\alpha_K}{1+\alpha} \omega_K \cdot b_{xki} \cdot f_{at} \cdot N_o$$

f_{at} = correction for the Be window attenuation and the transparency of the detector to 20 keV photons (0.997) (9)

ε_i = detector efficiency for the i position

N_i = count rate of a calibrated source N_o in the i position

b_{xki} = geometric efficiency of the detector for the 20 keV K X-rays

This equation is valid for infinitely thin sources.

Radius correction is not necessary because VYNS sources and rhodium discs have the same size. The detector resolution (FWHM) for 20 keV photons was about 25%.

For a rhodium foil of finite thickness, there will be a decrease in the counting rate due to absorption and scattering within the foil.

$$N_i = F_{iself} \cdot \varepsilon_i \cdot N_o$$

F_{iself} is the self-absorption factor.

The exact calculation of the dependence of self-absorption on foil thickness (d) and counting geometry is rather difficult due to multiple interactions, but a rough approximation can be made assuming an exponential absorption coefficient, μ, independent of the depth from which the radiation emanates. An experimental method for self-absorption determination is to obtain an

absorption curve for the active material by adding more material of the same specific activity, A, to make a thicker foil. The activity A', of a foil of thickness, d, is:

$$A' = \frac{A}{\mu \cdot d}\left(1 - e^{-\mu \cdot d}\right)$$

where: μ = mass absorption coefficient for foil (cm^{-1})

It is possible to lump self-scattering, self-absorption, and back-scattering into a single correction, μ, for a specific foil thickness, mounting and geometrical arrangement in a particular counting system.

Here we determined the self-absorption factor by a simulatenous irradiation of a rhodium disc (10 mm diameter and 0.1 mm thickness, m $\sim$ 95 mg) and a disc (same size) of Al-Rh alloy (4% Rh by weight) in the reactor to ensure that each disc experienced the same specific activity. The self-absorption factor, F_{iself}, is the ratio between the activity of the rhodium disc and the alloy disc:

$$F_{iself} = \frac{N_{i\,Rh}}{N_{i\,alloy} \cdot K_i}$$

K_i = correction due to absorption in the alloy

The rhodium self-absorption correction in the alloy was found by calculation to be less than 1% (assuming an $\bar{\mu}_{Rh} = 13.5 \frac{cm^2}{g}$) .

This was verified experimentally by relative activity determinations with and without rhodium absorbers of different thicknesses between source and detector for the 4 detector-to-source distances. The same procedure was performed for absorption of the 20 keV photons in aluminium absorbers of different thicknesses.

The results of F_{iself} are summarized in Table I.

Determination of α, α_K and the conversion ratio R.

The internal conversion coefficients α and α_K of the 39.75 keV transition in $^{103}Rh^m$ were determined from data shown in Fig. 1, the X-ray and γ-ray pulse height distributions were obtained from a $^{103}Rh^m$ source prepared from an elution of the Pd-Rh generator and detected by the NaI(Tl) crystal. The area of the pertinent peaks in the spectra at 20 and 40 keV were determined and corrected for any background present. From the following formula the absolute number of 40 keV photons was determined:

$$N_{40} = \frac{1}{1+\alpha} b_\gamma \cdot F_{escape} \cdot f_{at} \cdot N_o$$

F_{escape} = the iodine X-ray escape correction factor

b_γ = solid angle geometric efficiency of the NaI(Tl) crystal

N_o = disintegration rate of the source

f_{at} = correction for Be-window attenuation and the transparency of the detector to 40 keV photons (0.997)

To determine F_{escape} an absorber of stainless steel (0,5 mm) and aluminium (0,2 mm) was placed between the detector and source so that the 20 keV photons and the produced 6.4 keV X-rays were almost all absorbed. Fig. 2 shows such a spectrum. From the peak area ratio, one obtains directly the escape correction factor:

$$F_{escape} = \frac{F_{40}}{F_{11} + F_{40}} = 0.797 \pm 0.016$$

This value is in very good agreement with reported data (17). The solid angle geometric efficiency $b_\gamma = 0{,}0684 \pm 0{,}0004$ for a collimator of 2 cm diameter was calculated. The calculation was verified to within 0,5% by measurement with several collimators of different diameters using ^{103}Pd sources.

For five $^{103}Rh^{m}$ sources from different generator elutions a mean value

$$\alpha = 1531 \pm 30$$

was obtained at the 95% confidence level.

From the ratio of the two peak areas (20 keV and 40 keV) in Fig. 1, the K-internal conversion coefficient $\alpha_K = \frac{e_K}{\gamma}$ can be obtained.

$$\alpha_K = \frac{N_{20} \cdot F_{escape}}{N_{40} \cdot \omega_K}$$

N_{20}, N_{40} = peak area for the 20 (40) keV peak corrected (background and attenuation)

ω_k = 0.807 ± 0.031 (18)

From different generator elutions five $^{103}Rh^{m}$ sources were prepared and measured, from which a mean value

$$\alpha_K = 127 \pm 6$$

was obtained. This is in good agreement with the predicted theoretical value of 140 (19). The uncertainty of the α_K value is mostly due to $\Delta\omega_K$ (18).

In Table II data reported in the literature are presented with our results. From our results, a conversion ratio

$$R = \frac{\alpha_K}{\alpha_L + \alpha_M + \ldots} = 0,0914 \pm 0,0043 \text{ was calculated.}$$

For long-term control of the equipment, several ^{103}Pd sources were calibrated in the rhodium counter and measured before each day's experiment. The ^{103}Pd half-life used was 16.96 ± 0.06 days (16).

In each experiment several rhodium activity determinations were performed. The counting rate at time zero was obtained using $T_{1/2}$ = 56,116 min and the

least square method. This was an additional check that the equipment was working properly.

ACKNOWLEDGEMENT

We wish to thank Dr. H. Houtermans for interesting discussions during the course of these measurements and also to thank Dr. E. Kerö (IAEA) for his assistance with the electronic equipment.

References

1. TREBILCOCK, R.J., Neutron Dosimetry, Vol.1, p. 565, IAEA, Vienna (1963)
2. BRISBOIS, J., CAMPAN, J.-L., KO, P. and LERIDON, A., Bull.Inform. Sci.Tech. 81, 85 (1964)
3. VUORINEN, A., Standardization of Radionuclides, p. 257, IAEA, Vienna (1967)
4. NAGEL, W. and ATEN, A.H.W.,Jr., J.Nucl.Energy A/B 20, 475 (1966)
5. BRESESTI, A.M., BRESESTI, M. and NEUMANN, H., J.Inorg.Nucl.Chem. 29, 15 (1967)
6. BUTLER, J.P. and SANTRY, D.C., Nuclear Cross Sections and Technology, Vol.2, p. 803. NBS Spec.Publ.299, National Bureau of Standards, Washington (1968)
7. KIMURA, I., KOBAYASHI, K. and SHIBATA, T., J.Nucl.Sci.Tech. 6, 485 (1969)
8. THORNGATE, J.H., BROWN, M.D., DAVY, D.R., JOHNSON, D.R., PERDUE, P.T., SAIGUSA, T. and WAGNER, E.B., Oak Ridge National Laboratory, Rept. ORNL-4168, 193 (1967)
9. ING, H. and CROSS, W.G., JARI 24 (1973) p. 437
10. CZOCK, K.H., HASELBERGER, N., IAEA/RL/16-10-1973
11. OFFORI, E.D., CZOCK, K.H., IAEA/RL/24-3-1974
12. ING, H. and CROSS, W.G., Health Physics 25 (1973) 291
13. VLASOV, M.F., DUNFORD, C.L., SCHMIDT, J.J. and LEMMEL, H.D., INDC(NDS)-47/L
14. GÜNTHER, E.R., KNAUF, K., WALZ, K.F., JARI 24 (1973) 87
15. CZOCK, K.H., HOUTERMANS, H., IAEA/RL/14-1973
16. CZOCK, K.H., HASELBERGER, N., REICHEL, F. and POPA, S., IAEA/RL/21-1-1973
17. CROUTHAMEL, C.E., ADAMS, F. and DAMS, R., Applied Gamma-Ray Spectrometry (1970) 213
18. BAMBYNEK, W., Proceedings of the Intern.Conference on inner shell ionisation phenomena and future applications (1972) CONF-720404 Vol.1, p.80
19. HAGER, R.S., SELTZER, E.C., Nuclear Data A4 (1968) 59
20. KONDAIH, E., Phys.Rev. 79 (1950) 891
21. CORK, J.M., LeBLANC, J.M., STUMPF, F.B., NESTLER, W.H., Phys.Rev. 86 (1951) 575
22. AVIGNON, P., MICHALOWICZ, A., BOUCHEZ, R., J.Phys.Radium 16 (1955) 404
23. DRABKIN, G.M., ORLOV, V.I., RUSINOV, L.I., Isvest.Akad.Nauk SSSR, Ser. Fiz. 19 (1955) 324
24. BRESESTI, A.M., BRESESTI, M., NEUMANN, H., J.Inorg.Nucl.Chem. 29 (1967) 15
25. DeRAAD, B., MIDDELKOOP, W.C., VAN NOOYEN, B., ENDT, P.M., Physica XX (1954) 1278
26. LEPRI, M.A., LYON, W.S., JARI 20 (1969) 297
27. PAZSIT, A., CSIKAI, J., Journ. of Nucl.Phys. (UdSSR) 15 (1972) 412
28. HEGEDUS, F., Thesis, unpublished
29. NIESCHMIDT, E.B., PEARSON, D.A., JN-1218, p.87 and p. 122

TABLE I Detector parameters

Position	Detector-to-source distance [mm]	ε_i [%]	F_{iself}	$\varepsilon_i F_{iself}$	K_i
1	2.7	3.065 ± 0.015			
2	12.6	1.600 ± 0.006	0.436 ± 0.002	$6.93 \cdot 10^{-3}$	0.923 ± 0.003
3	22.8	0.835 ± 0.004	0.466 ± 0.002	$3.89 \cdot 10^{-3}$	0.935 ± 0.003
4	52.9	0.220 ± 0.002	0.482 ± 0.002	$1.06 \cdot 10^{-3}$	0.937 ± 0.003

TABLE II $^{103}Rh^{m}$ internal conversion coefficients values

Source	Conversion ratio, R	α_K/α	α_K
Kondiah[20]	0.20 ± 0.04	0.17 ± 0.04	
Cork et al.[21]	0.10 ± 0.04	0.076 ± 0.04	
Avignon et al.[22]	0.09 ± 0.01	0.069 ± 0.01	
Drabkin et al.[23]	0.18 ± 0.03	0.129 ± 0.03	
Bresesti et al.[24]	0.0986 ± 0.0050	0.0865 ± 0.005	
De Raad et al.[25]	0.098 ± 0.005	0.089 ± 0.005	
Vuorinen[3]	0.105 ± 0.01	0.0955 ± 0.010	
Ing et al.[9]	0.095 ± 0.005	0.0865 ± 0.0055	
Lepri[26]			180 ± 20
Pazsit et al.[27]			235 ± 15
Hegedus[28]	0.116 ± 0.030	0.131 ± 0.030	
Nieschmidt et al.[29]			138 ± 5
Theoretical value[19]			140 ± 20
Present work	0.0914 ± 0.0043	0.0826 ± 0.0050	127 ± 6

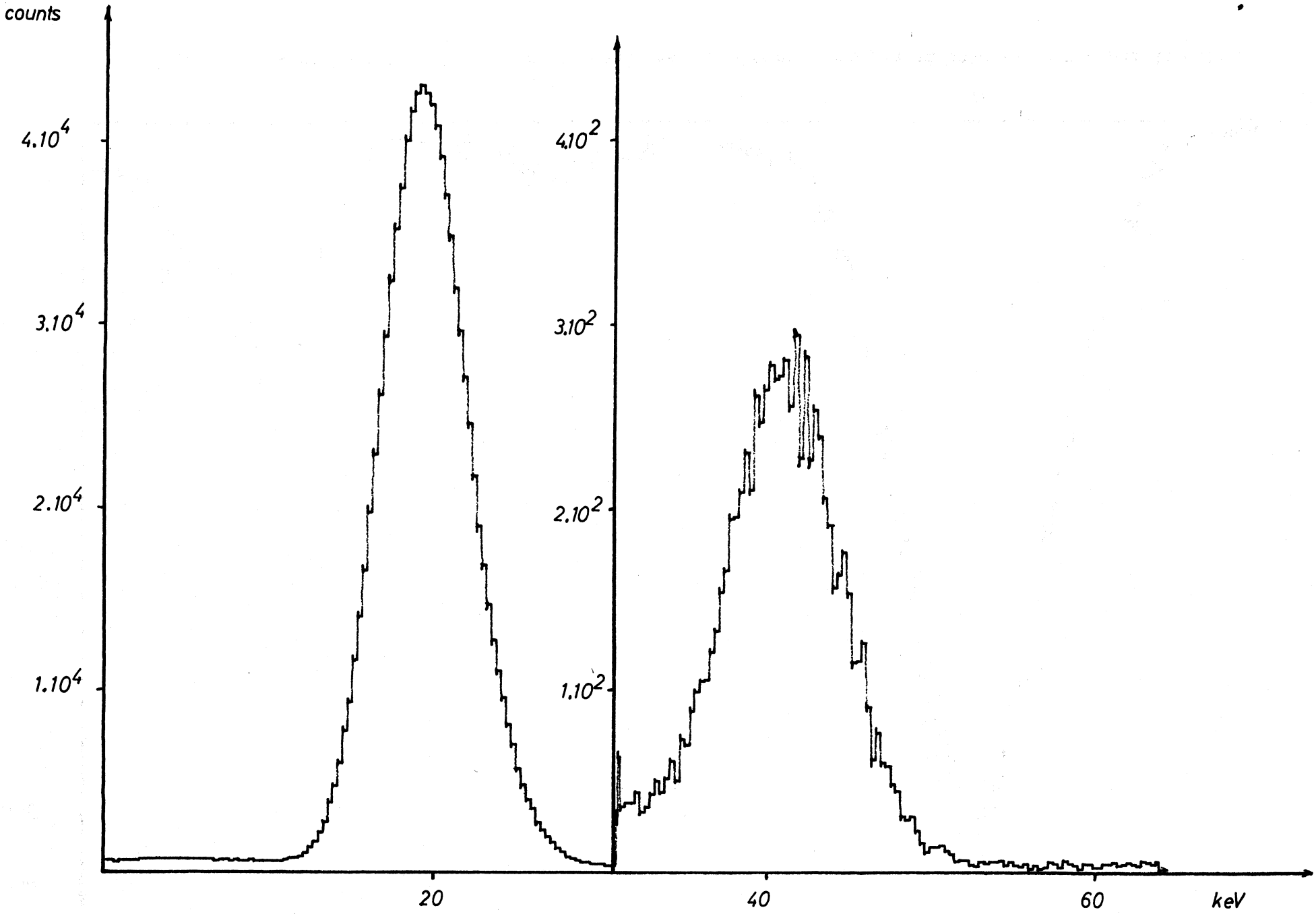

Fig. 1 Pulse height distribution obtained from a $^{103}Rh^{m}$ source.

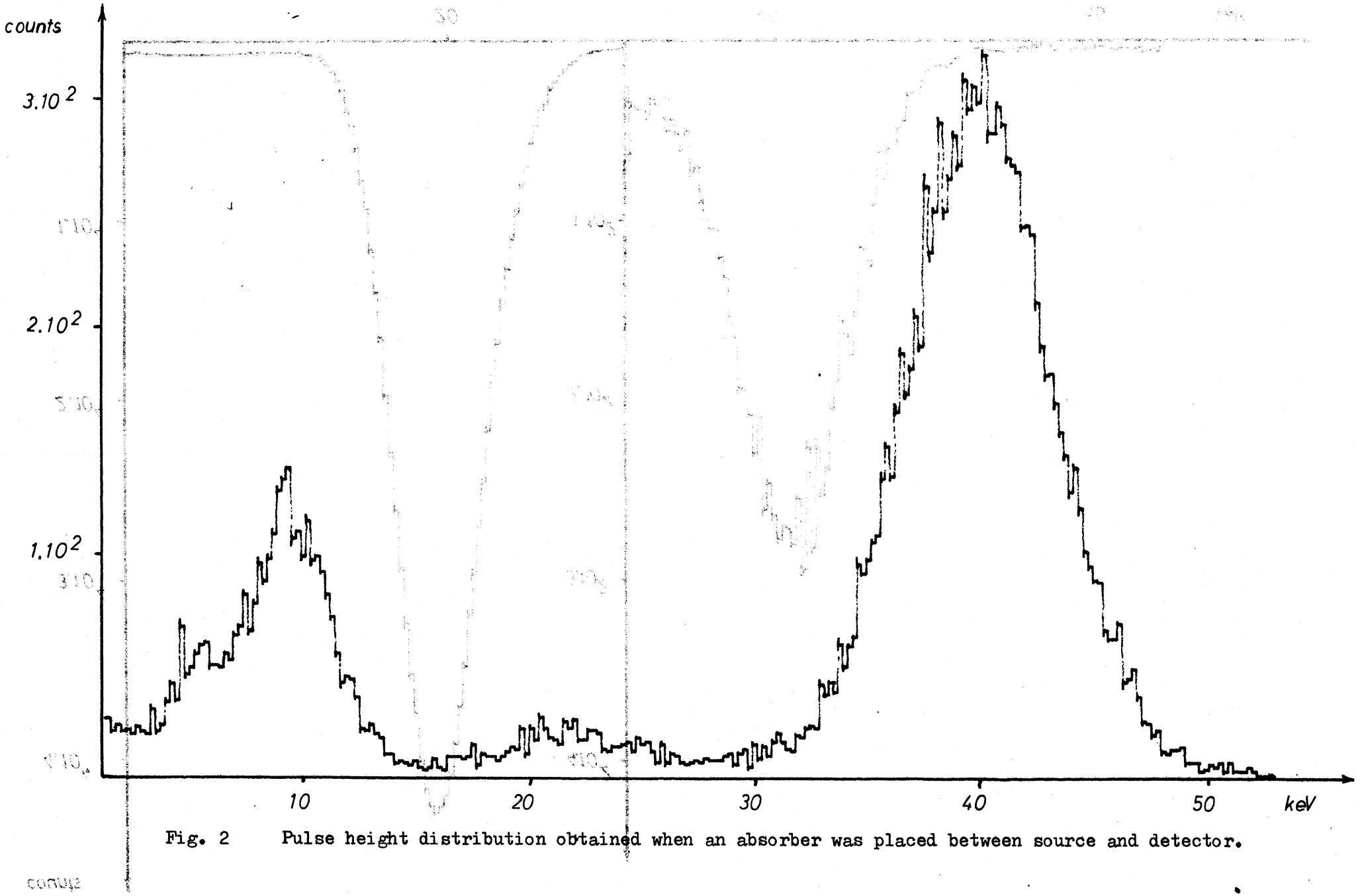

Fig. 2 Pulse height distribution obtained when an absorber was placed between source and detector.